A New Approach to Studying Microcapsule Wall Growth Mechanisms

Jian Li,[†] Adam P. Hitchcock,[†] Harald D. H. Stöver,*[,†] and Ian Shirley[‡]

BIMR and Deptartment of Chemistry, McMaster University, Hamilton, ON, Canada L8S 4M1, and Syngenta, Jealott's Hill International Research Centre, Bracknell, Berkshire RG42 6EY, United Kingdom

Received September 18, 2008; Revised Manuscript Received January 16, 2009

ABSTRACT: Polyurea microcapsules were prepared by sequential interfacial reaction of different aromatic and aliphatic isocyanates. The resulting composite capsule walls were studied using scanning transmission X-ray microscopy (STXM) to quantitatively map the distributions of the resulting aromatic and aliphatic polyureas across the capsule wall. Application of this method to both cross-linked and non-cross-linked polyurea capsules resulted in observation of different capsule wall growth mechanisms, depending mainly on the choice of monomers.

1. Introduction

Microcapsules are small, hollow devices designed to protect their contents from environmental degradation and to control the rate of release. Most microcapsules are prepared by interfacial polyaddition of oil-soluble polyisocyanates dispersed in water, with aqueous polyamines, though analogous approaches are used to form polyurethane and polyamide capsules. The resulting spherical polymer capsules typically contain an organic active or fill, such as insect pesticides or pheromones, inks, and fragrances, and are mainly used in agriculture, carbonless papers applications, and personal care products. Recent applications involve capsules as catalyst supports[1,2] and in display devices.[3,4]

Understanding the mechanisms of capsule wall formation and growth is key to controlling wall strength and permeability and hence to improving capsule performance, especially in terms of variable release[5] and release triggered by acid[6] or base.[7] The two major wall growth mechanisms are the moving boundary mechanism[8] and the stationary boundary mechanism, both illustrated in Figure 1. Pearson and Williams[5] determined that the reaction zone in interfacial encapsulations often moves during the reaction, with the water-soluble monomer diffusing through the initially formed polymer film to reach and react with the oil-soluble monomer, building up successive layers on the interior capsule wall. This model has been used by many researchers to interpret the encapsulation processes for polyurethane, polyurea, and polyamide microcapsules.[9−14] In contrast, the stationary boundary mechanism invokes the presence of a stable, stationary reaction zone during the encapsulation process (Figure 1b). Under this mechanism, capsule wall thickness does not increase with time once the initial polymer film has been formed, though its density may change.

Encapsulation processes can be affected by many factors, including the polarity, diffusion coefficients and reactivities of monomers, the polarity and permeability of the forming polymers, solvent polarity, solution pH, and temperature. While a better understanding of the encapsulation process could lead to improved capsule design, experimental studies of the encapsulation process have been complicated by the high rate of interfacial polymerizations and the typically submicron thickness of the wall.

Janssen and co-worker[12] used narrow-disperse capsules prepared from 2,4-toluene diisocyanate (TDC) and diethylenetriamine (DETA) with diameters varying from 3 to 5 mm to study the wall formation process experimentally. They found that the capsule wall thickness increased with reaction time, in agreement with the moving boundary mechanism. In contrast, Jabbari,[15] studying smaller microcapsules prepared from hexamethylene diisocyanate (HMDI) and hexamethylenediamine (HMDA), found that capsule wall thickness did not increase with time once the initial polymer film had been formed, implying that the boundary is stationary in this system.

We aim to design an effective approach to studying polyurea capsule wall composition and wall formation mechanism. Our strategy involves using mixed isocyanate monomers of different reactivity in the organic or fill phase and studying their sequential interfacial polyaddition with aqueous amines to form composite polyurea capsules. The spatial distribution of the different isocyanate residues across the capsule wall should then reflect the capsule wall formation process.[16] We are using scanning transmission X-ray microscopy (STXM) to map the distribution of these different monomers across the capsule wall with submicron spatial resolution.

We demonstrate here a strategy to study interfacial encapsulation processes and determine the growth processes in two types of polyurea capsules as a function of cross-linking and polymerization temperature. Our approach involves using mixtures of aromatic and aliphatic isocyanates in an oil phase consisting mainly of *p*-xylene. Aromatic isocyanates are known to be significantly more reactive than their aliphatic counterparts.[17,18] Sato reported the rates of phenyl isocyanate with methanol to be 50 times higher than the rate of reaction of ethyl isocyanate with methanol.[19] Kuck et al. reported the reaction of HMDI with secondary amines to be about an order of magnitude lower than the corresponding reaction of TDI.[20] Competitive interfacial polyaddition of a mixture of aromatic and aliphatic isocyanates should thus lead to sequential incorporation of these two isocyanates. If the rate-limiting step is diffusion of the aqueous amine into the oil phase, then the polyurea formed early should be rich in aromatic residues, while polyurea formed later should be rich in aliphatic groups. Hence, observation of an aromatic/aliphatic composition gradient across the capsule walls would indicate that wall formation involves a moving reaction zone or boundary (Figure 1a), as the wall grows toward the interior of the capsule. Conversely, absence of such a compositional gradient would imply wall formation with a fixed though broad reaction zone, leading to an interpenetrating network (IPN) of sequentially formed aromatic and aliphatic polyureas, as illustrated in Figure 1b.

We compared two types of polyurea microcapsules, both based on mixtures of aromatic and aliphatic isocyanates, but

* To whom correspondence should be addressed.
[†] McMaster University.
[‡] Syngenta, Jealott's Hill International Research Centre.

10.1021/ma802130n CCC: $40.75
Published on Web 03/13/2009

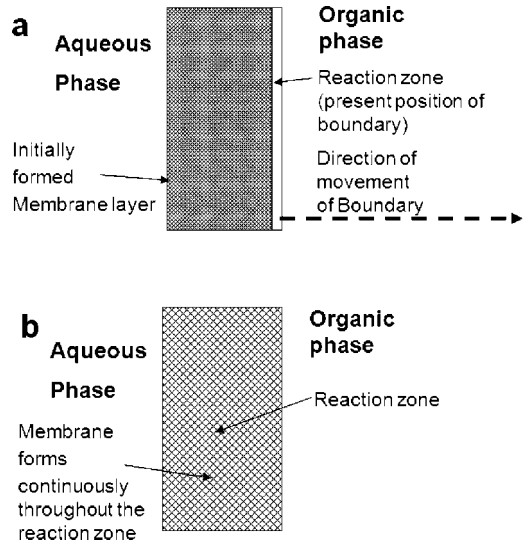

Figure 1. Illustration of two different mechanisms proposed for capsule wall formation: (a) moving boundary mechanism; (b) stationary boundary mechanism.

with different degrees of cross-linking. **PID** capsules (**P**MPPI + **I**PDI/**D**ETA) are formed by reaction of mixtures of polymethylene polyphenylene isocyanate (PMPPI) and isophorone diisocyanate (IPDI), with diethylenetriamine (DETA) as aqueous amine. **MHH** capsules (**M**DI + **H**MDI/**H**MDA) are formed by reaction of methylene diphenyl 4,4′-diisocyanate (MDI) and hexamethylene diisocyanate (HMDI), with aqueous hexamethylenediamine (HMDA). PMPPI and MDI are two aromatic isocyanates commonly used for preparing microcapsules. They have similar reactivities toward polyamines, but only PMPPI acts as a cross-linker. IPDI and HMDI are aliphatic isocyanates commonly used for their UV resistance and serve as aliphatic markers in this study. DETA and HMDA are widely used polyamines, with DETA being more polar and also acting as a cross-linker.

2. Experimental Section

2.1. Sample Preparation. The interfacial polymerizations were carried out in a jacketed glass reactor fitted with an overhead stirrer. A mixture of 1 g of aromatic and 1 g of aliphatic isocyanate dissolved in a total of 10 mL of *p*-xylene was dispersed into 35 mL of 1 wt % aqueous PVA solution at about 800 rpm for 15 min. Then 1.5 equiv of polyamine, on an amino group per isocyanate group basis, in 5 mL of 1 wt % PVA solution was added to the emulsion. Different polymerization temperatures were employed as described below. The obtained capsules were washed on a Buchner vacuum filter with water and tetrahydrofuran to remove residual aqueous amine and extract the oil phase, respectively. They were subsequently dried under vacuum to constant weight. For TEM and STXM analysis, dried capsules were embedded in an epoxy resin prepared by mixing trimethylolpropane triglycidyl ether (TTE) and 4,4′-methylenebis(2-methylcyclohexylamine) (MBMCA) in a 1:1 weight ratio and cured at 70 °C for 3 days. This epoxy showed superior radiation resistance compared to the commonly used Spur epoxy and does not contain carbonyl and phenyl groups that might interfere with the spectral analysis. The embedded samples were ultramicrotomed to about 100 nm thickness.

2.2. Scanning Transmission X-ray Microscopy. Scanning transmission X-ray microscopy (STXM) at the dedicated polymer STXM beamline 5.3.2 of the Advanced Light Source (ALS) was used to map the distribution of aromatic and aliphatic polyureas across the capsule wall. STXM is a microscopy-based version of near-edge X-ray absorption fine structure (NEXAFS) spectroscopy,[21] combining good energy resolution of about 0.1 eV with spatial resolution of about 50 nm. Our previous results have shown

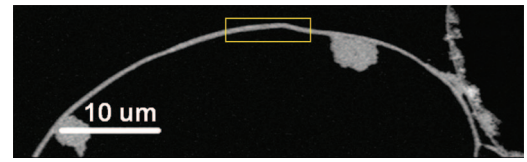

Figure 2. STXM overview image (optical density) at 285.2 eV, of **PID** capsule wall prepared at 50 °C. The yellow rectangle indicates the area where the image sequence for Figure 4 was recorded.

that STXM is a powerful tool for microcapsule studies.[22−24] For measurement, a 100 nm thick microtomed section of capsules embedded in epoxy resin is imaged with a monochromatic X-ray beam, and a sequence of images are taken over a range of X-ray energies covering the C 1s spectral region. The data analysis is carried out using the program aXis2000.[25] It involves a pixel-by-pixel fit of the image sequence to quantitative C 1s reference spectra for the pure aromatic and aliphatic polyureas as well as the epoxy resin. The fit coefficients are then assembled into individual component maps, and color-coded composite maps are further constructed by mapping each component to one of the three primary colors (in this work we assign red to epoxy, green to aromatic, and blue to aliphatic). STXM can easily distinguish between aromatic and aliphatic polyurea, based on the strong C 1s $\rightarrow \pi^*$ absorption band present only in the aromatic urea 285 eV. Both ureas have strong C 1s $\rightarrow \pi^*$ absorption bands near 289.4 eV (carbonyl bands), while the epoxy resin was designed to not have any aromatic and carbonyl groups so as not to interfere with the urea analysis.[18]

3. Results and Discussion

First we examined the **PID** capsules prepared from PMPPI + IPDI//DETA at constant temperature of 50 °C for 24 h. Figure 2 shows a STXM image of a partial wall cross section taken at 285.2 eV, the energy of maximum contrast of capsules to the epoxy resin.

Figure 3 shows the chemical structures for IPDI, MDI, and PMPPI as well as reference spectra for the three components present in the microtomed capsule wall sections: aromatic polyurea (green), aliphatic polyurea (blue), and epoxy (red).[26]

The reference spectrum for the epoxy resin was obtained directly from each sample to account for minor differences in curing between samples, while the spectra for the two types of polyurea were obtained from model polyureas and capsules.[26] These three reference spectra were used to analyze the image sequence obtained for the boxed area indicated in Figure 2. Singular value decomposition (SVD)[26] resulted in the component maps and the color-coded composite map shown in Figure 4. Integrations across the boxed area in Figure 4b resulted in composition profiles across the capsule wall shown in Figure 4c. STXM provides quantitative composition information, with good spatial resolution. The capsules shown here have thin and dense walls due to use of the poor solvent *p*-xylene and the high cross-linking ability of the PMPPI used as major wall former.

There is a slight compositional gradient across the capsule wall, with aromatic polyurea more prevalent in the outer layer and aliphatic polyurea enriched in the inner layer, in accordance with their expected sequential incorporation into the wall, as described earlier.[26] Here we are interested in exploring the mechanistic implications of this compositional gradient in terms of wall formation and cross-linking. The presence of this gradient indicates that the reaction zone moves during the encapsulation process. It starts with the formation of mainly aromatic polyurea in the outer shell layer and moves inward as conversion shifts to the less reactive aliphatic isocyanate. The line-out across the capsule wall (Figure 4c) shows these gradients. The wall segment studied further reveals low conversion of IPDI, with a ratio of aromatic/aliphatic urea of 10:1.

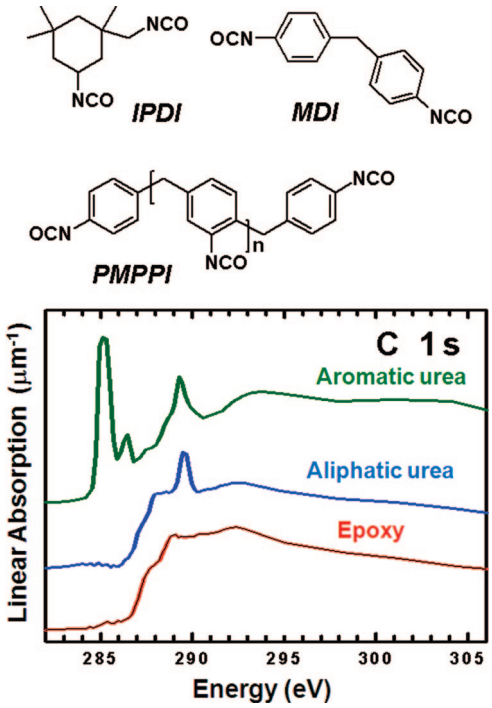

Figure 3. Chemical structures of IPDI, MDI, and PMPPI and reference spectra for the three chemical components of the samples: embedding epoxy, aliphatic polyurea, and aromatic polyurea. The spectra were placed on absolute intensity scales by scaling to match the elemental response outside of the near-edge region and vertically offset for clarity.

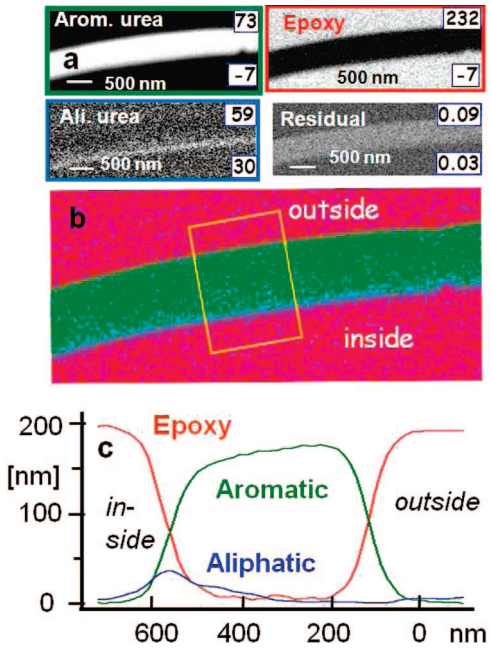

Figure 4. (a) Individual component maps of of aromatic urea, aliphatic urea, and epoxy resin, for the wall section of the **PID** capsule shown in Figure 2, prepared at 50 °C. (b) Color-coded composite map of the same three components. (c) Component profiles (in nanometer thickness) across the capsule wall (orange box).

We attribute this low conversion of IPDI to the low permeability to amine of the cross-linked aromatic polyurea formed at 50 °C in *p*-xylene, a poor solvent for polyurea, as well as to the lower reactivity of the IPDI compared to the aromatic isocyanate, PMPPI.

Subsequently, we carried out polymerizations using the same protocol but at room temperature, designed to lead to less dense

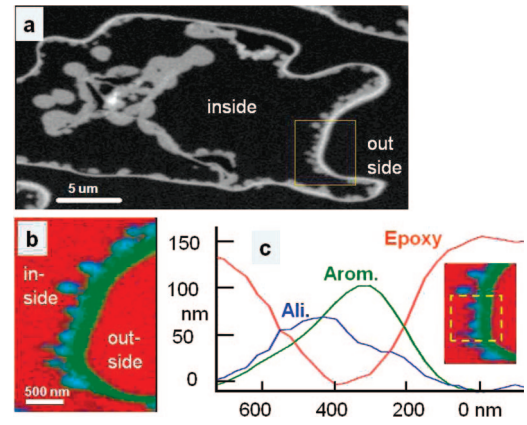

Figure 5. Chemical mapping of **PID** capsule wall prepared at room temperature: (a) STXM image taken at 285.2 eV; (b) chemical mapping the wall of **PID** capsule; (c) plot of averaged component profiles across the component maps.

aromatic polyurea walls and hence increase the in-diffusion of IPDI. Figure 5a−c shows the STXM results obtained for **PID** capsules formed at room temperature after 24 h.

The STXM image taken at 285.2 eV (Figure 5a) shows an overall image of a capsule embedded in epoxy. Typical for such capsules, the outside surface templated by the oil−water interface is much smoother than the inside surface. The color-coded compositional map is shown in Figure 5b while component across-wall profiles are shown in Figure 5c. The latter were obtained by rotating the component maps and summing multiple horizontal line profiles (yellow box in the inset to Figure 5c) to improve statistics. This analysis confirms that the outer layers are rich in aromatic polyurea while the inner bulbous features are deposits or growths that are rich in aliphatic polyurea. These aliphatic bulbs may reflect the presence of pores in the aromatic outer shell that admit amine. The large aggregates seen in the center of the capsule in Figure 5a are attributed to aggregates of mainly aliphatic polyurea formed in the interior of the capsule. The wall segment studied shows comparable levels of aromatic and aliphatic polyurea being produced at this stage of the encapsulation.

To try to further enhance the conversion of IPDI in these **PID** capsules, we used a two-stage thermal profile consisting of 24 h at room temperature followed by another 24 h at 70 °C (Figure 6a). This polymerization protocol had been shown earlier to lead to two-layer walls.[26]

The high conversion of aliphatic isocyanate in that case indicated that the aromatic polyurea formed at room temperature during the first 24 h is more permeable, allowing continued diffusion of DETA into the reaction zone. The subsequent temperature increase to 70 °C should also facilitate diffusion of DETA through the capsule wall and ensure high conversion of the less reactive isocyanate, IPDI. Figure 6b shows a STXM image taken at 285.2 eV, at the end of the 48 h reaction. At this energy only the aromatic polyurea is seen since it is the only species with significant absorption (see Figure 3). The STXM compositional maps and across-wall profiles (Figure 6c,d) for the **PID** system prepared by this two-stage polymerization confirm the overall aromatic/aliphatic wall gradient, indicating a moving boundary mechanism. The wall segment studied shows high conversion of IPDI, comparable to that of PMPPI, suggesting that the aromatic polyurea walls formed at room temperature are less dense and permit subsequent aliphatic polyurea wall growth.

Both at 25 and 50 °C, all **PID** capsules show compositional gradients across the capsule walls, which indicates that the overall wall formation mechanism does not change over this temperature

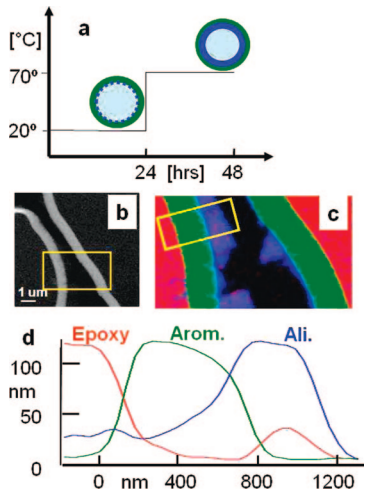

Figure 6. Chemical mapping of **PID** capsule wall prepared using the two-stage temperature process: (a) STXM image taken at 285.2 eV; (b) chemical mapping the wall of **PID** capsule; (c) plot of averaged profiles across the component maps.

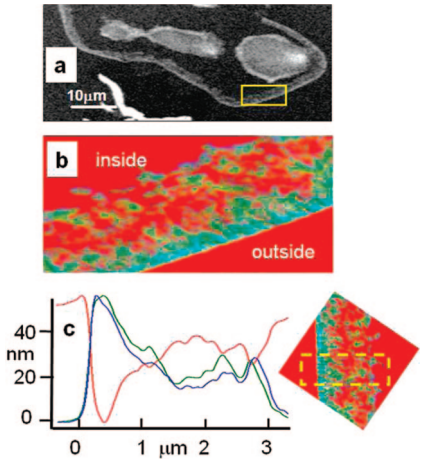

Figure 7. Chemical mapping of **MHH** capsule wall prepared using the two-stage temperature process: (a) STXM image taken at 285.2 eV; (b) chemical mapping the **MHH** capsule wall; (c) plot of averaged profiles across the component maps.

regime. Changing the temperature does appear to change the density of the initially formed aromatic polyurea capsule wall, which affects the subsequent rate of growth of aliphatic polyurea capsule wall.

To explore the effect of different levels of cross-linking on the wall structure and on the wall formation mechanism, we studied **MHH** capsules composed of MDI + HMDI//HMDA, both using the two-stage temperature process, and at constant 50 °C. Both processes produce **MHH** capsules with very porous walls (Figures 7 and 8) and without large-scale aromatic/aliphatic compositional gradients across the walls. In both cases aromatic and aliphatic polyurea densities decrease in parallel from the outer to the inner wall surface, suggesting formation of an interpenetrating network (IPN) structure. This is attributed to wall growth according to the stationary boundary mechanism, where the HMDA keeps diffusing into the organic phase to react with MDI and HMDI subsequently in a broad but static reaction zone. From wall segment studies we also observed that the **MHH** capsules formed with the two-stage temperature process show a higher aromatic to aliphatic ratio compared to that of **MHH** capsules made from constant 50 °C. We again attribute this difference to the formation of a denser polyurea skin at 50 °C which slows the diffusion of HMDA and affects conversion of especially HMDI.

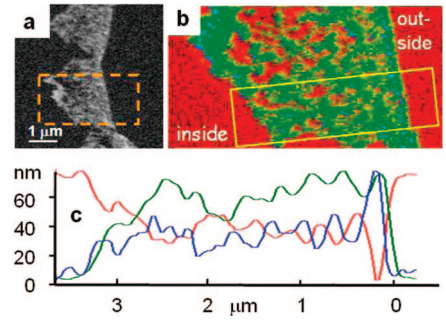

Figure 8. Chemical mapping of **MHH** capsule wall made from constant temperature of 50 °C: (a) STXM image taken at 285.2 eV; (b) chemical mapping the wall of **MHH** capsule; (c) plot of averaged profiles across the component maps.

Comparison of these two systems indicates that the capsule wall formation can change dramatically with the cross-linking ability and the polarity of the monomers used. Changing the temperature does not fundamentally change the wall formation mechanism but affects the densities of the capsule walls. Dense capsule walls would limit the diffusion of either isocyanates or polyamines, leading to lower conversion of the less reactive isocyanates. Similarly, wall density would affect release of the active fill material.

4. Conclusion

Capsule wall morphologies and growth mechanisms in polyurea capsules prepared using mixtures of isocyanates have been studied by STXM. Highly cross-linked, dense PMPPI + IPDI//DETA (**PID**) capsules are shown to grow by the moving boundary mechanism, while their less cross-linked and less dense MDI + HMDI//HMDA (**MHH**) analogues are shown to grow by a stationary boundary process. This approach of studying interfacial polymerization is not limited to polyurea capsules but may be useful in mechanistic studies of other interfacial systems.

This information can help guide the design of new capsules, depending on release and strength properties required. Capsule walls formed from highly cross-linking monomers, resulting in moving boundary mechanism, would tend to result in slowly releasing walls. If higher mechanical wall strength is required for such capsules, one answer could be to use a combination of highly cross-linking aromatic isocyanates to form the release-controlling outer skin by the moving boundary mechanism, with less reactive and aliphatic isocyanates to form a permeable inner support membrane by the stationary boundary mechanism.

Acknowledgment. Research was supported by Syngenta, NSERC, Canada Foundation for Innovation, and the Canada Research Chair program. STXM was performed at beamline 5.3.2 at the Advanced Light Source, Berkeley, CA, which is supported by U.S. Department of Energy under Contract DE-AC03-76SF00098. We thank David Kilcoyne and Tolek Tyliszczak for their excellent support of the instrument and Sander Reijerkerk and Padraic Foley for some of the sample preparation and STXM data analysis. We thank Marcia West for her excellent job on sample ultramicrotoming.

References and Notes

(1) Ramarao, C.; Ley, S. V.; Smith, S. C.; Shirley, I. M.; DeAlmeida, N. *Chem. Commun.* **2002**, *10*, 1132.
(2) Price, K. E.; Mason, B. P.; Bogdan, A. R.; Broadwater, S. J.; Steinbacher, J. L.; McQuade, D. T. *J. Am. Chem. Soc.* **2006**, *128*, 10376.
(3) Comiskey, B.; Albert, J. D.; Yoshizawa, H.; Jacobson, J. *Nature (London)* **1998**, *394*, 253.

(4) Yoshizawa, H. *KONA* **2004**, *22*, 23.
(5) Scher, H. B.; Van Koppenhagen, J. E.; Shirley, I. M.; Follows, R.; Wade, P.; Earley, F. G. P.; Shirley, D. B. WO 2001019509 A1.
(6) Van Koppenhagen, J. E.; Scher, H. B.; Lee, K.-S.; Shirley, I. M.; Wade, P.; Follows, R. WO 0005952, **2000**.
(7) Van Koppenhagen, J. E.; Scher, H. B.; Lee, K.-S.; Lee, C. C.; Shirley, I. M.; Wade, P.; Follows, R. US Patent 2002037306 A1.
(8) Stadelhofer, J. W.; Zellerhoff, R. B. *Chem. Ind. (London)* **1989**, *7*, 208.
(9) Pearson, R. G.; Williams, E. L. *J. Polym. Sci., Polym. Chem. Ed.* **1985**, *23*, 19.
(10) Sirdesai, M.; Khilar, C. *Can. J. Chem. Eng*. **1988**, *66*, 509.
(11) Yadav, S. K.; Suresh, A. K.; Khilar, K. C. *AIChE* **1990**, *36*, 431.
(12) Janssen, L.; Nijenhuis, K. T. *J. Membr. Sci.* **1992**, *65*, 59.
(13) Yadav, S. K.; Khilar, K. C.; Suresh, A. K. *AIChE J.* **1996**, *42*, 2616.
(14) Kubo, M.; Harada, Y.; Kawatsu, T.; Yonemoto, T. *J. Chem. Eng. Jpn.* **2001**, *34*, 1506.
(15) Jabbari, E. *J. Microencapsulation* **2001**, *18*, 801.
(16) Croll, L. M.; Morin, C.; Koprinarov, I.; Hitchcock, A. P.; Stöver, H. D. H. *J. Phys. IV* **2003**, *104*, 507.
(17) Hong, K.; Park, S. *Mater. Sci. Eng.* **1999**, *A272*, 418.
(18) Sultan, W.; Busnel, J.-P. *J. Therm. Anal. Calorim.* **2006**, *83*, 355.
(19) Sato, M. *J. Org. Chem.* **1962**, *27*, 819.
(20) Kuck, M.; Balle, G.; Slawyk, W. *Analyst* **1999**, *124*, 933.
(21) Stöhr, J. *NEXAFS Spectroscopy*; Springer Tracts in Surface Science 25; Springer: Berlin, 1992.
(22) Croll, L. M.; Stöver, H. D. H.; Hitchcock, A. P. *Macromolecules* **2005**, *38*, 2903.
(23) Hitchcock, A. P.; Morin, C.; Zhang, X.; Araki, T.; Dynes, J. J.; Stöver, H. D. H.; Brash, J. L.; Lawrence, J. R.; Leppard, G. G. *J. Electron Spectrosc.* **2005**, *144*−*147*, 259.
(24) Hitchcock, A. P.; Stöver, H. D. H.; Croll, L. M.; Childs, R. F. *Aust. J. Chem.* **2005**, *58*, 423.
(25) aXis2000 is written in Interactive Data Language (IDL). It is available free for non-commercial use from http://unicorn.mcmaster.ca/aXis2000.html.
(26) Hitchcock, A. P.; Li, J.; Reijerkerk, S.; Foley, P.; Stöver, H. D. H.; Shirley, I. M. *J. Electron Spectrosc. Relat. Phenom.* **2007**, *156*, 467.

MA802130N